Inorganic Chemistry
Article

Inorg. Chem. **2010**, *49*, 2479–2485 **2479**
DOI: 10.1021/ic902392y

Oxovanadium(IV) Silsesquioxane Complexes

Christian Ohde,[†] Christian Limberg,*[,†] Reinhard Stösser,[†] and Serhiy Demeshko[‡]

[†]*Institut für Chemie, Humboldt-Universität zu Berlin, Brook-Taylor-Strasse 2, 12489 Berlin, Germany, and* [‡]*Institut für Anorganische Chemie, Georg-August-Universität Göttingen, Tammannstrasse 4, 37077 Göttingen, Germany*

Received December 3, 2009

In the context of a potential modeling of reduced oxovanadium species occurring on the surfaces of silica-supported vanadia catalysts in the course of its turnover, the incompletely condensed silsesquioxane $H_3{}^{c\text{-pentyl}}\mathbf{T_7}$ was reacted with $Cl_4V(THF)_2$ (where THF = tetrahydrofuran) in the presence of triethylamine. Precipitation of 3 equiv of $HNEt_3Cl$ seemed to point to the clean formation of $[(^{c\text{-pentyl}}\mathbf{T_7})(V^{IV}Cl)]$ (**1**), which was supported by electron paramagnetic resonance studies performed for the resulting solutions, but further analytical and spectroscopic investigations showed that the processes occurring at that stage are more complex than that and even include the formation of $[(^{c\text{-pentyl}}\mathbf{T_7})(V^{V}O)]_2$ as a side product. Storage of a red-brown hexane solution of this product mixture reproducibly led to the precipitation of blue crystals belonging to the chloride-free compound $[(^{c\text{-pentyl}}\mathbf{T_7})_2(V^{IV}{=}O)_3(THF)_2]$ (**2**), as revealed by single-crystal X-ray diffraction. Performing the same reaction in the presence of 2 equiv of pyridine leads to an analogous product, where the THF ligands are replaced by pyridine. Subsequent investigations showed that the terminal oxo ligands at the vanadium centers are, on the one hand, due to the presence of adventitious water; on the other hand, the $[^{c\text{-pentyl}}\mathbf{T_7}]^{3-}$ ligand also acted as a source of O^{2-}. The results of SQUID measurements performed for **2** can be interpreted in terms of a ferromagnetic coupling between the vanadyl units. Exposing **2** to a dioxygen atmosphere resulted in its immediate oxidation to yield the V^V complex $[(^{c\text{-pentyl}}\mathbf{T_7})(V^{V}O)]_2$, which may model a fast reoxidation reaction of oxovanadium(IV) trimers on silica surfaces.

Introduction

Various different surface species have been discussed as being active during the V_2O_5/SiO_2-catalyzed oxidative dehydrogenation (ODH) of light alkanes and methanol in one way or another,[1] and their structural motifs motivate attempts to mimic them in molecular compounds.[2,3] The construction of molecular models for metal oxo surface sites requires ligands that are capable of mimicking the oxidic environments that metal oxo moieties experience on oxidic support or bulk materials, and in this context in particular, two ligand systems have established themselves: silsesquioxanes[4,5] and calixarenes.[6] For the modeling of oxovanadium(V) sites, we have successfully employed both,[2,7,8] and this work contributes to the silsesquioxane chemistry.

Incompletely condensed silsesquioxanes are probably the most realistic low-molecular-weight models for silica surface silanols because they possess both structural and electronic similarities.[9] Their reaction with transition-metal precursors thus resembles the grafting process applied for the preparation of heterogeneous catalysts, and the resulting complexes have proven to be promising both as homogeneous catalysts and as precursors for highly efficient metal-based heterogeneous catalysts.[10]

Feher and co-workers have intensely investigated the coordination chemistry of deprotonated $H_3{}^{R}\mathbf{T_7}$ (Chart 1) and also with respect to V^V centers.[5] They were able to synthesize a mononuclear complex $^{R}\mathbf{I}$ (with R = cyclohexyl)

*To whom correspondence should be addressed. E-mail: christian.limberg@chemie.hu-berlin.

(1) A classification of the literature according to the suggested active oxo species is reviewed in: Fu, H.; Liu, Z.-P.; Li, Z.-H.; Wang, W.-N.; Fan, K.-N. *J. Am. Chem. Soc.* **2006**, *128*, 11114–11123.
(2) Hoppe, E.; Limberg, C.; Ziemer, B. *Inorg. Chem.* **2006**, *45*, 8308–8317.
(3) Canny, J.; Thouvenot, R.; Tézé, A.; Hervé, G.; Leparulo-Loftus, M. *Inorg. Chem.* **1991**, *30*, 967.
(4) (a) Copéret, C.; Chabanas, M.; Saint-Arroman, R. P.; Basset, J.-M. *Angew. Chem., Int. Ed.* **2003**, *42*, 156–181. (b) Meurig Thomas, J.; Raja, R.; Lewis, D. W. *Angew. Chem., Int. Ed.* **2005**, *44*, 6456–6482. (c) Zeller, J.; Treptow, J.; Radius, U. *Z. Anorg. Allg. Chem.* **2007**, *633*, 741–746.
(5) Feher, F. J.; Walzer, J. F. *Inorg. Chem.* **1991**, *30*, 1689–1694.
(6) (a) Homden, D. M.; Redshaw, C. *Chem. Rev.* **2008**, *108*, 5086–5130. (b) Limberg, C. *Eur. J. Inorg. Chem.* **2007**, 3303–3314. (c) Mendoza-Espinosa, D.; Hanna, T. A. *Inorg. Chem.* **2009**, *48*, 7452–7456.
(7) Ohde, C.; Brandt, M.; Limberg, C.; Döbler, J.; Ziemer, B.; Sauer, J. *Dalton Trans.* **2008**, 326–331.
(8) (a) Hoppe, E.; Limberg, C.; Ziemer, B.; Mügge, C. *J. Mol. Catal.* **2006**, *251*, 34–40. (b) Hoppe, E.; Limberg, C. *Chem.—Eur. J.* **2007**, *13*, 7006–7016.
(9) (a) Duchateau, R. *Chem. Rev.* **2002**, *102*, 3525–3542. (b) Lorenz, V.; Edelmann, F. T. *Z. Anorg. Allg. Chem.* **2004**, *630*, 1147–1157. (c) Feher, F. J.; Budzichowski, T. A. *Polyhedron* **1995**, *14*, 3239–3253. (d) Lovat, S.; Mba, M.; Abbenhuis, H. C. L.; Vogt, D.; Zonta, C.; Licini, G. *Inorg. Chem.* **2009**, *48*, 4724–4728.
(10) Wada, K.; Mitsudo, T. *Catal. Surv. Asia* **2005**, *9*, 229–241.

Published on Web 01/29/2010

Chart 1. Equilibrium between ^{R}**I** and ^{R}**II**

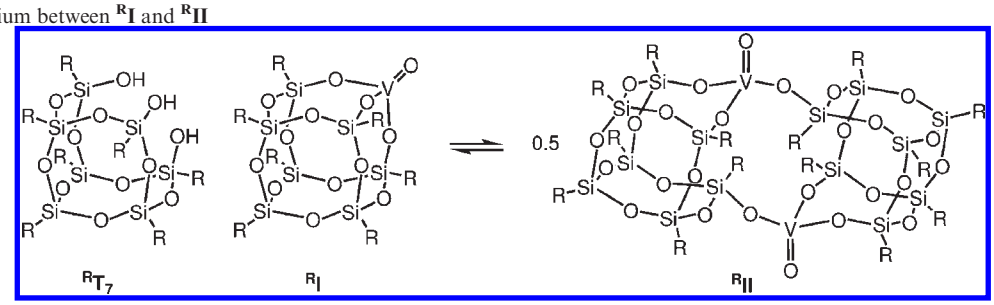

Chart 2. Oxovanadium(V) Silsesquioxane Complexes

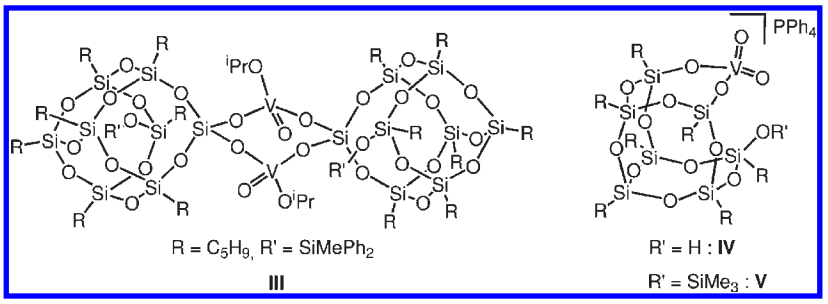

and found that in solution it forms an equilibrium with a dimeric version, ^{R}**II**, in which each vanadium atom is bonded to oxygen atoms of two different T_7 cages (see Chart 1). Derivatives of ^{R}**I** with R = cyclopentyl and isobutyl have also been synthesized.[10,11] While the system **I**/**II** was found to be a poor oxidation catalyst under thermal conditions, it was reported to be active as a catalyst for photooxidations.[12] The complex **I**/**II**, originally synthesized in 1991, remained the only known oxovanadium silsesquioxane complex until recently, when we described novel V^{V} derivatives whose formation processes, structures, and spectroscopic properties provided helpful information concerning the analysis and assignment of surface species (see Chart 2).[7]

While the oxidation state of the vanadium centers within compounds **I**−**V** is V+, naturally there is also interest in reduced complexes that could model reduced species formed after oxidation reactions on V_2O_5/SiO_2 catalyst surfaces, and in this context, V^{IV} and V^{III} are important. We therefore decided to investigate the chemistry of V^{IV} on an oxo surface modeled by $^{c\text{-pentyl}}$**T**$_7$ in order to study the behavior of the resulting complexes and possible reoxidation reactions.

Experimental Section

Materials and Methods. $H_3{}^{c\text{-pentyl}}\mathbf{T}_7$ and $VCl_4(THF)_2$ (where THF = tetrahydrofuran) were synthesized according to reported procedures.[13,14] In the case of $H_3{}^{c\text{-pentyl}}\mathbf{T}_7$, the white solid obtained was subjected to an additional purification step: it was suspended in Et_2O and stirred over 2 days at room temperature. After filtration, it was dried overnight under a high vacuum. All experiments were carried out in a dry argon atmosphere using a glovebox and/or standard Schlenk techniques. Microanalyses were performed on a Leco CHNS-932 or HEKAtech EURO elemental analyzer. IR spectra were recorded using samples prepared as KBr pellets with a Shimadzu FTIR 8400S Fourier transform infrared spectrometer. Magnetic data were measured with a Quantum-Design MPMS-5S SQUID magnetometer at 0.5 T in the range from 2 to 295 K. The powdered samples were contained in a gel bucket and fixed in a nonmagnetic sample holder. Electron spin resonance (ESR) spectra were measured on an ERS 300 (ZWG/Magnettech GmbH, Berlin-Adlershof, Germany).

Reaction of $H_3{}^{c\text{-pentyl}}\mathbf{T}_7$ with $VCl_4(THF)_2$. A total of 0.50 g (0.57 mmol) of $H_3{}^{c\text{-pentyl}}\mathbf{T}_7$ and 192 mg (0.57 mmol) of $VCl_4(THF)_2$ were dissolved in 20 mL of THF, and 0.40 mL (2.85 mmol) of NEt_3 was added. The red-brown reaction mixture was stirred overnight at room temperature. Subsequently, all volatiles were removed under reduced pressure. After drying of the residue for 3 h under a high vacuum, it was extracted with 20 mL of hexane. The residue was washed twice with 5 mL of Et_2O. After drying overnight under a high vacuum, 240 mg (1.75 mmol, 3 equiv) of NEt_3HCl was obtained. All volatiles were removed from the hexane extract, and the crude material was dried under a high vacuum, yielding in 520 mg of a gray, slightly reddish powder. Elem anal. Found: C, 46.14; H, 7.02; N, 0.12; Cl, 2.21. Anal. Calcd for $\mathbf{1}_{0.65}(^{c\text{-pentyl}}\mathbf{I}/^{c\text{-pentyl}}\mathbf{II})_{0.35}(C_6H_{14})_{0.6}$: C, 46.19; H, 7.17; N, 0.00; Cl, 2.30. The presence of residual hexane has been confirmed by ^{1}H NMR.

Synthesis of 2. A total of 0.50 g (0.57 mmol) of $H_3{}^{c\text{-pentyl}}\mathbf{T}_7$ and 192 mg (0.57 mmol) of $VCl_4(THF)_2$ were dissolved in 15 mL of THF, and 0.40 mL (2.85 mmol) of NEt_3 was added. The red-brown reaction mixture was stirred overnight at room temperature. Afterward, the reaction mixture was connected to a Schlenk tube filled with degassed distilled water and stirred for 1.5 h (transport of water through the gas phase). Subsequently, all volatiles were removed under reduced pressure. After drying of the residue for 3 h under a high vacuum, it was extracted with 20 mL of hexane. The resulting solution was filled into a test tube and stored in the glovebox. Over 1 week, blue crystals were obtained by slow evaporation of the solvent. Separation and drying of the crystalline material under reduced pressure yielded in 130 mg (0.06 mmol) of **2** (η = 33%). IR (KBr, cm^{-1}): 2950 s, 2865 m, 1452 m, 1246 m, 1110 sh, 1090 vs, 1048 sh, 1021 m, 976 m, 876 m, 848 s, 727 vw, 598 w, 541 m, 494 m. Anal. Calcd for $C_{78}H_{142}O_{29}Si_{14}V_3$ (2087.5): C, 44.83; H, 6.85. Found: C, 45.12; H, 6.90.

(11) Carniato, F.; Boccaleri, E.; Marchese, L.; Fina, A.; Tabuani, D.; Camino, G. *Eur. J. Inorg. Chem.* **2007**, 585–591.
(12) Wada, K.; Nakashita, M.; Yamamoto, A.; Wada, H.; Mitsudo, T. *Chem. Lett.* **1997**, 1209–1210.
(13) Feher, F. J.; Budzichowski, T. A.; Blanski, R. L.; Weller, K. J.; Ziller, J. W. *Organometallics* **1991**, *10*, 2526–2528.
(14) Heyn, B.; Hiplar, B.; Kreisel, G.; Schreer, H.; Walther, D. *Anorganische Synthesechemie*, 2nd ed.; Springer-Verlag: Berlin, 1986; p 20.

Table 1. Crystallographic Data and Experimental Details for **2** and **3**

	2	**3**
molecular formula	$C_{78}H_{142}O_{29}Si_{14}V_3$	$C_{80}H_{136}N_2O_{27}Si_{14}V_3$
fw	2090.0	2103.99
temp (K)	100(2)	100(2)
wavelength (Å)	0.710 73	0.710 73
system, space group	*Pbcn*	*Pbcn*
a (Å)	25.9729(5)	26.065(6)
b (Å)	19.5740(4)	19.569(5)
c (Å)	20.5865(5)	20.655(5)
α (deg)	90	90
β (deg)	90	90
γ (deg)	90	90
U (Å^3)	10466.0(4)	10536(4)
Z	4	4
ρ (g cm^{-3})	1.326	1.326
μ (mm^{-1})	0.492	0.488
F(000)	4428	4444
cryst size (mm^3)	0.32 × 0.28 × 0.24	0.50 × 0.30 × 0.25
2*θ* range (deg)	2.57−25.25	2.56−27.00
reflns collected/unique [R_{int}]	21 820/9458 [R_{int} = 0.0611]	120 751/11 493 [R_{int} = 0.1468]
completeness to *θ* (%)	99.8	99.8
refinement method	full-matrix least squares on F^2	full-matrix least squares on F^2
data/restraints/param	9455/0/570	11 493/0/569
GOF on F^2	1.226	1.160
final *R* indices [$I > 2\sigma(I)$]	R1 = 0.1052, wR2 = 0.2268	R1 = 0.0999, wR2 = 0.2527
R indices (all data)	R1 = 0.1173, wR2 = 0.2309	R1 = 0.1314, wR2 = 0.2637
largest diff peak and hole (e Å^{-3})	0.590 and −0.648	0.665 and −0.727

Scheme 1. Synthesis of **2** and **3**

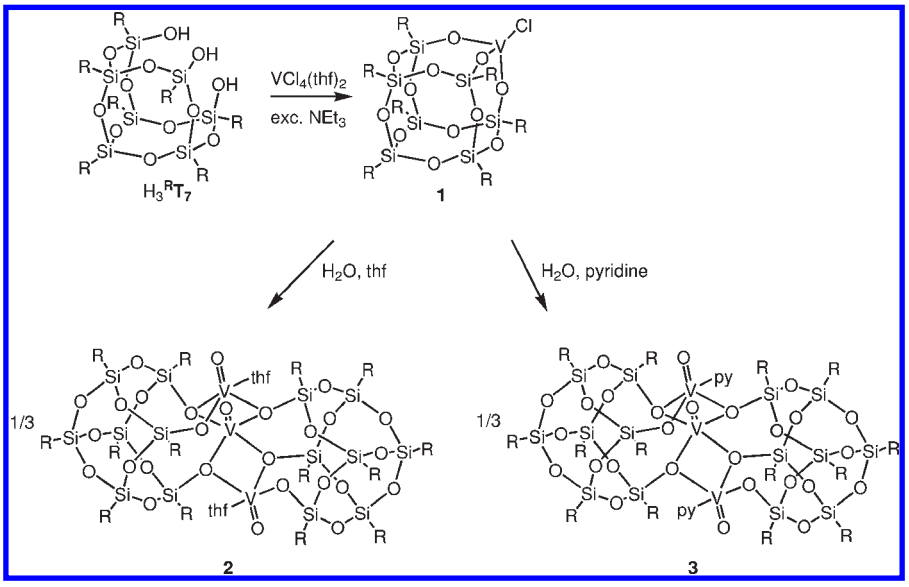

Synthesis of 3. A total of 0.50 g (0.57 mmol) of $H_3^{c\text{-pentyl}}\mathbf{T_7}$ and 192 mg (0.57 mmol) of $VCl_4(THF)_2$ were dissolved in 15 mL of THF. Afterward, 0.40 mL (2.85 mmol) of NEt_3 and 31 μL (0.33 mmol) of pyridine were added. The red-brown reaction mixture was stirred overnight at room temperature. Afterward, the reaction mixture was connected to a Schlenk tube filled with degassed distilled water and stirred for 1.5 h (transport of water through the gas phase). Subsequently, all volatiles were removed under reduced pressure. After drying of the residue for 3 h under a high vacuum, it was extracted with 20 mL of hexane. The resulting solution was filled into a test tube and stored in the glovebox. Over 1 week, blue crystals were obtained by slow evaporation of the solvent. Separation and drying of the crystalline material under reduced pressure yielded 127 mg (0.06 mmol) of **3** (η = 32%). IR (KBr, cm^{-1}): 2950 s, 2865 m, 1608 w, 1448 m, 1245 m, 1110 vs, 1088 vs, 1047 sh, 1020 m, 1013 m, 974 m, 854 s, 756 w, 728 vw, 698 w, 579 w, 543 s, 485 m. Anal. Calcd for $C_{80}H_{136}N_2O_{29}Si_{14}V_3$ (2101.4): C, 45.68; H, 6.52; N, 1.33. Found: C, 45.86; H, 6.69; N, 1.01.

X-ray Crystallography. Crystallographic data and experimental details of the data collection for **2** (CCDC 755731) and **3** (CCDC 755730) are summarized in Table 1. The crystals were mounted on a glass fiber and then transferred into the cold nitrogen gas stream of the Stoe IPDS diffractometer using Mo Kα radiation. The structure was solved by direct methods (*SHELXS-97*)[15] and refined versus F^2 (*SHELXL-97*)[16] with anisotropic temperature factors for all non-hydrogen atoms. All hydrogen atoms were added geometrically and refined using a riding model.

Results and Discussion

Complex Synthesis and Structures. Bearing in mind that compounds of the type [$^{\mathbf{R}}\mathbf{T_7}Ti^{IV}X$] (X = OEt, O^{i}Pr, O^{i}Bu,

(15) Sheldrick, G. M. *SHELXS-97, Program for Crystal Structure Solution*; University of Göttingen: Göttingen, Germany, **1997**.

(16) Sheldrick, G. M. *SHELXL-97, Program for Crystal Structure Refinement*; University of Göttingen: Göttingen, Germany, **1997**.

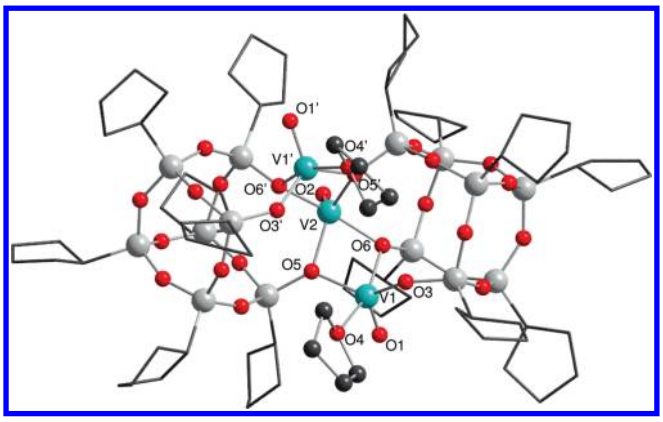

Figure 1. Molecular structure of **2**. Hydrogen atoms are omitted for clarity. Selected bond lengths and atom distances (Å): V1−O1, 1.586(5); V2−O2, 1.590(8); V1−O3, 1.873(6); V1−O4, 2.116(5); V1−O5, 2.008(5); V1−O6, 2.008(5); V2−O5, 1.997(5); V2−O6, 2.022(5); V1−V2, 3.0659(17).

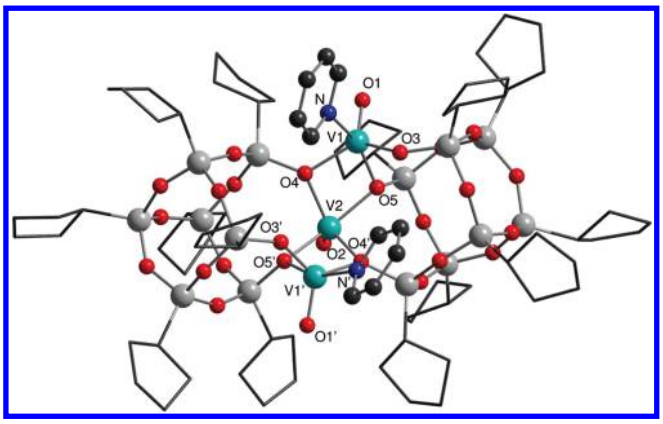

Figure 2. Molecular structure of **3**. Hydrogen atoms are omitted for clarity. Selected bond lengths and atom distances (Å): V1−O1, 1.589(4); V2−O2, 1.572(6); V1−O3, 1.876(4); V1−O4, 2.010(4); V1−O5, 2.027(4); V1−N, 2.128(5); V2−O4, 2.013(4); V2−O5, 2.025(4); V1−V2, 3.0828(13).

CH_2Ph, NMe_2) are readily accessible from reactions of $H_3{}^{R}\mathbf{T_7}$ and TiX_4,[17] $H_3{}^{c\text{-pentyl}}\mathbf{T_7}$ dissolved in THF was treated with equimolar amounts of $Cl_4V(THF)_2$ in the presence of excessive triethylamine with the aim of preparing an analogous compound [$^{c\text{-pentyl}}\mathbf{T_7}V^{IV}Cl$] (**1**; see Scheme 1).

This led to the immediate precipitation of ca. 3 equiv of NEt_3HCl and a red-brown solution, which remained optically unchanged within 24 h (also after separation of NEt_3HCl). All attempts to crystallize the product, which on the basis of the amount of precipitated NEt_3HCl was assumed to correspond mainly to **1**, failed. In order to further investigate the contents of this solution, NMR, electron paramagnetic resonance (EPR), and elemental analyses were performed. The ^{51}V NMR spectroscopic investigation, surprisingly, revealed that $^{c\text{-pentyl}}\mathbf{I}/^{c\text{-pentyl}}\mathbf{II}$ containing V^V centers was part of the product mixture. Subsequently, the solution was studied by EPR spectroscopically. At 293 K, the eight-line spectrum expected for a single mononuclear V^{IV} complex was observed, and this remained unchanged for 3 days. Variation of the temperature and solvent led to changes suggesting a monomer/dimer equilibrium for this complex (see the Supporting Information).

Hence, NMR spectroscopy has evidenced the presence of $^{c\text{-pentyl}}\mathbf{I}/^{c\text{-pentyl}}\mathbf{II}$, while EPR proved the formation of a V^{IV} species that might correspond to **1**, differing from $^{c\text{-pentyl}}\mathbf{I}/^{c\text{-pentyl}}\mathbf{II}$ in the chloride content. After removal of all volatiles, an elemental analysis of the residue revealed a chloride content of 2.21%, which would point to a $^{c\text{-pentyl}}\mathbf{I}/\mathbf{1}$ ratio of 35/65%, assuming that these are the sole species within the product mixture. Redissolution in *n*-hexane and storage of the resulting red-brown solution led to the precipitation of blue crystals. These were composed of the trinuclear compound [$(^{c\text{-pentyl}}\mathbf{T_7})_2(V^{IV}{=}O)_3(THF)_2$] (**2**; 17% yield), as evidenced by a single-crystal X-ray diffraction study. The molecular structure is shown in Figure 1.

The molecule shows a crystallographic C_2 symmetry; i.e., V1 and V1′ are related by a C_2 axis going through the atoms V2 and O2. Every vanadium atom is coordinated by five oxygen atoms, one of which is doubly bound (O1 and O2). In principle, this could result in two different coordination geometries: A trigonal bipyramid or a square pyramid. Because it is usually hard to distinguish between those, the parameter τ was calculated.[18] This showed that the situation for the V1/V1′ atoms is right in between both structural types ($\tau = 0.5$), whereas the coordination environment around V2 is approximately trigonal-bipyramidal ($\tau = 0.7$). The bond lengths are in the usual ranges observed for V−O bonds. The V=O bond lengths are almost identical with those observed for $^{c\text{-hexyl}}\mathbf{II}$, while the V1−O3 bond [1.873(6) Å] is about 0.1 Å longer than the corresponding bonds in $^{c\text{-hexyl}}\mathbf{II}$. As expected, the distances between V1 to O5 and O6 (2.00 Å) belonging to bridging siloxide functions are even longer. The distance between V1 and O4 amounts to 2.116(5) Å, which is typical for THF molecules coordinating to vanadium centers.[19,20]

With regard to the outcome of this experiment, it was repeated in the presence of 0.66 equiv of pyridine to see whether this leads to an analogous pyridine complex. Indeed, [$(^{c\text{-pentyl}}\mathbf{T_7})_2(V^{IV}{=}O)_3(py)_2$] (**3**) was isolated with a crystalline yield of 18%. Not surprisingly, the molecular structure of **3**, as depicted in Figure 2, is very similar to that of **2**. Even the distance of the vanadium atom to the coordinating pyridine molecule [2.128(5) Å] is comparable to the V1···THF distance [2.116(5) Å] in **2**.

Magnetism. **2** and **3** contain three d^1 metal centers, which, in principle, could be coupled in various ways. To investigate that, a variable-temperature SQUID measurement was performed for **3** (Figure 3).

Magnetic susceptibility data were measured from powdered samples of solid material in the temperature range

(17) (a) Edelmann, F. T.; Giessmann, S.; Fischer, A. *J. Organomet. Chem.* **2001**, 80–89. (b) Duchateau, R.; Abbenhuis, H. C. L.; van Santen, R. A.; Meetsma, A.; Thiele, S. K.-H.; van Tol, M. F. H. *Organometallics* **1998**, *17*, 5663–5673. (c) Crocker, M.; Herold, R. H. M.; Orpen, A. G. *Chem. Commun.* **1997**, 2411–2412. (d) Viotti, O.; Seisenbaeva, G. A.; Kessler, V. G. *Inorg. Chem.* **2009**, *48*, 9063–9065.

(18) Addison, A. W.; Nageswara Rao, T.; Reedijk, J.; van Rijn, J.; Verschoor, G. C. *J. Chem. Soc., Dalton Trans.* **1984**, 1349–1356.

(19) Priebsch, W.; Rehder, D. *Inorg. Chem.* **1990**, *29*, 3013–3019.

(20) Thiele, K.; Görls, H.; Imhof, W.; Seidel, W. *Z. Anorg. Allg. Chem.* **1999**, *625*, 1927–1933.

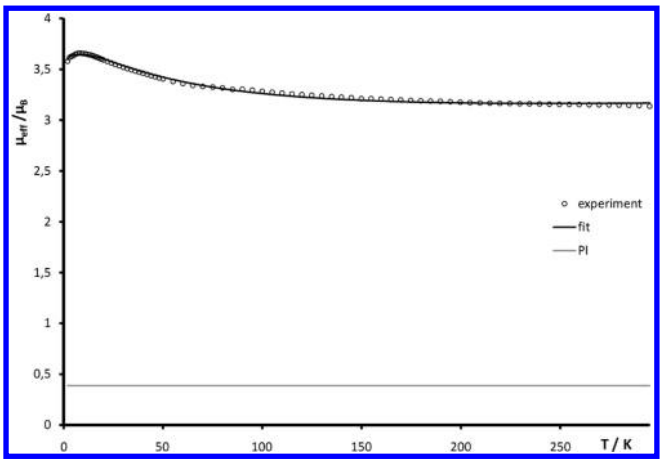

Figure 3. Plot of μ_{eff} versus temperature for **3**.

295−2 K using a SQUID magnetometer (MPMS-5, Quantum Design) at an applied magnetic field of 0.5 T. According to the molecular structure of **3**, lacking any atoms directly bridging the vanadium centers V1 and V1′, only two equal interaction pathways should be considered. The appropriate Heisenberg−Dirac−van Vleck spin Hamiltonian includes one isotropic exchange coupling constant $J = J_{12} = J_{23}$ and Zeeman splitting (eq 1).[21]

$$\hat{H} = -2J(\hat{S}_1\hat{S}_2 + \hat{S}_2\hat{S}_3) + g\mu_B B\sum_{i=1}^{3}\hat{S}_{zi} \qquad (1)$$

A Curie-behaved paramagnetic impurity (PI) with spin $S = 1.5$ and temperature-independent paramagnetism (TIP) was included according to $\chi_{calc} = (1 - PI)\chi + PI\chi_{mono} + TIP$. The calculated curve fit is shown as a solid black line in Figure 3. The fitting[22] of the experimental data over the full temperature range for **3** with the spins $S_1 = S_2 = S_3 = {}^1/_2$ led to $J = 36\ cm^{-1}$ and $g_1 = g_2 = g_3 = 1.88$. The values for g_1, g_2, and g_3 are in the range commonly observed for V^{IV} atoms.[8,23] The positive coupling constant deduced as well as the image of the temperature dependence of the magnetic moment clearly indicates the presence of ferromagnetic exchange interactions between the V^{IV} centers. The coupling is probably mediated by the oxygen atoms of the silsesquioxane ligand bridging the vanadium centers.

Complex Formation. The vanadium centers of **2** and **3** contain terminal oxo ligands, and considering that $Cl_4V(THF)_2$ had been employed as the starting material, naturally the question concerning their origin arose. Because hydrolysis was an obvious possibility (although reagents, solvents, and the atmosphere had been dried rigorously), the influence of water was tested: 0.1−0.5 equiv of water was deliberately added to such reactions. It turned out that the presence of up to 0.1 equiv improved

Scheme 2. Water Elimination in $H_3{}^{R}\mathbf{T_7}$ Leading to $^{R}\mathbf{VI}$ (R = Cyclohexyl)

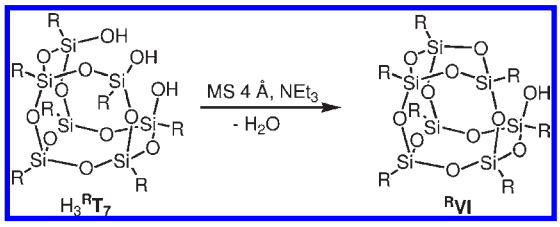

the yields by up to 23%, but beyond that, the yields decreased again, so that after the addition of 0.5 equiv all attempts to isolate **2** failed. Moreover, the ligand precursor $H_3{}^{c\text{-pentyl}}\mathbf{T_7}$ itself was considered as a possible source of the terminal oxo ligands. Feher and co-workers had reported in 1989 that in the case of the incompletely condensed silsesquioxane $H_3{}^{c\text{-hexyl}}\mathbf{T_7}$ intramolecular water elimination leading to $^{c\text{-hexyl}}\mathbf{VI}$ can occur upon heating or in the presence of 4 Å molecular sieves combined with traces of NEt_3 (see Scheme 2).[24] Furthermore, it was reported that such cyclodehydration reactions also occur when $H_3{}^{c\text{-hexyl}}\mathbf{T_7}$ is reacted with high-valent reagents such as MoO_2Cl_2 or $POCl_3$.[25]

Obviously, after the elimination of 3 equiv of NEt_3HCl, no protons are left within the system, but a similar rearrangement can also be imagined to occur after replacement of the protons by metal centers. Perhaps it takes place partially already in the course of the reaction of $VCl_4(THF)_2$ with $H_3{}^{c\text{-pentyl}}\mathbf{T_7}$.

Accordingly, an investigation to identify any $^{c\text{-pentyl}}\mathbf{VI}$ formed as a byproduct (in its deprotonated form or in the presence of moisture as such) was started. For this purpose, an experiment was performed as before, and after separation of the product crystals, the contents of the mother liquor were investigated by ^{29}Si NMR spectroscopy. Indeed, besides some weak signals, probably originating from $H_x{}^{c\text{-pentyl}}\mathbf{T_7}^{(3-x)-}$, a set of five signals at −55.3, −57.2, −65.8, −67.9, and 69.9 ppm with an intensity pattern that would fit to $^{c\text{-pentyl}}\mathbf{VI}$ were observed. The chemical shifts agree reasonably well with those reported in the literature for $^{c\text{-hexyl}}\mathbf{VI}$, but some of the signals deviate somewhat (possibly because of residual V^{IV} in the sample) so that the assignment was not unambiguous. In order to further support it, a hexane solution of the product was, first of all, exposed to air to protonate any siloxide functions; then it was treated with tetrabutylammonium vanadate and subsequently investigated by electrospray ionization mass spectrometry (ESI-MS). While any $H_x{}^{c\text{-pentyl}}\mathbf{T_7}^{(3-x)-}$ silsesquioxane compound containing two or more OH functionalities should react in a 1:1 stoichiometry to give a complex $[H_{x-2}{}^{c\text{-pentyl}}\mathbf{T_7}VO_2]^{(x-2)-}$ (for instance, $H_3{}^{R}\mathbf{T_7}$ yields $^{R}\mathbf{IV}$, R = cyclopentyl),[7] $^{c\text{-pentyl}}\mathbf{VI}$ has only one OH group and can thus lead to either **4** or **5** (see Scheme 3).

4 and **5** would give rise to peaks with *m*/*e* ratios of 955.2152 (found: *m*/*e* 955.2193) and 1795.4880 (found: *m*/*e* 1795.4986) in the ESI-MS spectrum, respectively, and

(21) Kahn, O. *Molecular Magnetism*; Wiley-VCH Publishers Inc.: New York, 1993.

(22) Simulations of the experimental magnetic data with a full-matrix diagonalization of exchange coupling and Zeeman splitting were performed with the *julX* program developed by E. Bill (Max Planck Institute for Bioinorganic Chemistry, Mühlheim/Ruhr, Germany).

(23) Theil, H.; Freiherr von Richthofen, C.-G.; Stammler, A.; Bögge, H.; Glaser, T. *Inorg. Chim. Acta* **2008**, *361*, 916–924.

(24) Feher, F. J.; Newman, D. A.; Walzer, J. F. *J. Am. Chem. Soc.* **1989**, *111*, 1741–1748.

(25) (a) Feher, F. J.; Rahimian, K.; Budzichowski, T. A.; Ziller, J. W. *Organometallics* **1995**, *14*, 3920–3926. (b) Feher, F. J.; Budzichowski, T. A.; Rahimian, K.; Ziller, J. W. *J. Am. Chem. Soc.* **1992**, *114*, 3859–3866.

Scheme 3. Reaction of ^{R}**VI** with Tetrabutylammonium Vanadate (R = Cyclopentyl)

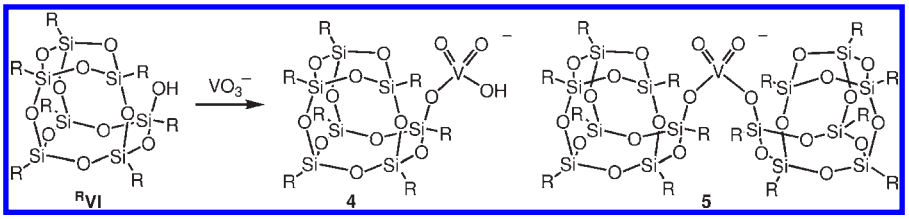

Chart 3. Proposed Vanadate Species on γ-Alumina Surfaces at Low Loading[26]

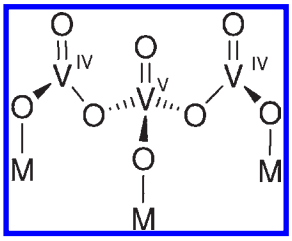

indeed such peaks were detected with the expected isotope patterns. While the peak at *m*/*e* 955.2193 could also be indicative of compound $^{c\text{-pentyl}}$**IV**, the one at *m*/*e* 1795.4986 is characteristic of **5** and thus strongly supports the formation of $^{c\text{-pentyl}}$**VI** as a side product. Consequently, the V=O groups within **2** and **3** partly also originate from $^{c\text{-pentyl}}\mathbf{T}_7^{3-}$. Because the above-mentioned experiments with added water did not lead to convincing results, the slow hydrolysis by traces of water was simulated by connecting the reaction vessel to a tube containing water vapor that was allowed to slowly diffuse through the junction. Indeed, that led to a significant increase in the yield to 33%, thus pointing to the relevance of traces of moisture for the formation of **2** and **3**.

Reactivity toward Dioxygen. The complexes **2** and **3** can be regarded as models for reduced oxovanadium "trimers" on silica supports. Beyond that, such trinuclear units have been suggested to be the predominant species in the case of low vanadium loadings on γ-alumina,[27] and it was found that even under oxidizing conditions only ~30% of the vanadium centers were in the oxidation state V+, whereas the majority was present as V^{IV} (Chart 3). Therefore, the reactivity of **2** toward dioxygen was of interest in the context of a potential modeling of the reoxidation step at catalyst surfaces and to investigate the behavior of such units in general. Indeed, the compounds are readily oxidized by dioxygen, both in the solid state and in solution. After exposure of **2** to a dioxygen atmosphere, the blue crystals became darker within 1 h.

Subsequently, a ^{51}V NMR spectrum revealed the characteristic signals of the V^{V} complexes ^{R}**I**/^{R}**II** (R = cyclopentyl). Besides, a further vanadium compound must have been formed, which could not be detected by ^{51}V NMR. An EPR measurement was performed that

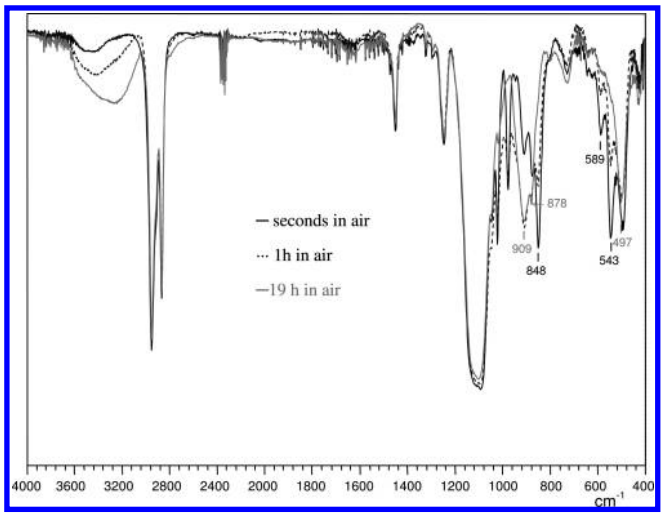

Figure 4. Exposure of **2** embedded in a KBr disk to air.

pointed to a mononuclear V^{IV} species in the solution, but, unfortunately, beyond that the byproduct could not be further characterized. The oxidation process could be monitored for **2** embedded in a KBr matrix: As shown in Figure 4, exposing a KBr disk of **2** to air leads to the disappearance of its characteristic IR bands, while new bands grow in that could be identified as belonging to ^{R}**I**/^{R}**II** by comparison with the IR spectrum of an authentic sample. Hence, the oxidation of $O{=}V^{2+}$ centers bound to a silsesquioxane ligand modeling a silica surface occurs very fast already at room temperature. This is consistent with the findings for supported oxovanadium species used for the ODH of propane: Reoxidation of those catalysts is fast in comparison to the reduction step involving propane dehydrogenation.[27]

Conclusions

The reaction between $H_3{}^{c\text{-pentyl}}\mathbf{T}_7$ and $Cl_4V(THF)_2$ leads to a product mixture containing $^{c\text{-pentyl}}$**I**/$^{c\text{-pentyl}}$**II** and a V^{IV} complex that might correspond to **1**. It will be interesting to test the in situ reactivity of such solutions in the future. While they are stable as such over longer periods of time, the contents dissolved in hexane proved to be extremely sensitive to hydrolysis and ligand decomposition: Contact with traces of moisture leads to the formation of trinuclear oxovanadium(IV) complexes $[(^{c\text{-pentyl}}\mathbf{T}_7)_2(V^{IV}{=}O)_3(L)_2]$ (L = THF, **2**; L = pyridine, **3**), whose vanadium centers are ferromagnetically coupled. Regarding these compounds as models for surface species formed on silica or other supports in the course of loading with vanadia as catalytically active "trimers", the reactivity in contact with dioxygen was of

(26) Klose, F.; Wolff, T.; Lorenz, H.; Seidel-Morgenstern, A.; Suchorski, Y.; Piórkowska, M.; Weiss, H. *J. Catal.* **2007**, *247*, 176–193.

(27) (a) Argyle, M. D.; Chen, K. D.; Iglesia, E.; Bell, A. T. *J. Phys. Chem. B* **2005**, *109*, 2414–2420. (b) Dinse, A.; Khennache, S.; Frank, B.; Hess, C.; Herbert, R.; Wrabetz, S.; Schlögl, R.; Schomäcker, R. *J. Mol. Catal. A* **2009**, *307*, 43–50.

interest, which indicated the facile oxidation of such units to V^V species.

Acknowledgment. We are grateful to the Deutsche Forschungsgemeinschaft, the CRC546, the Fonds der Chemischen Industrie, and the BMBF for financial support.

Supporting Information Available: EPR studies after the reaction of $H_3{}^{\text{c-pentyl}}\mathbf{T_7}$ with $VCl_4(THF)_2$, ESR spectra and simulation of **1** and **2**, ESR spectra of **2** after exposure to air, and IR spectra of $^{\mathbf{R}}\mathbf{II}$ and the oxidation product of **2** with dioxygen. This material is available free of charge via the Internet at http://pubs.acs.org.